Acta Med. Okayama, 2024
Vol. 78, No. 3, pp. 215–225

Acta Medica Okayama
http://escholarship.lib.okayama-u.ac.jp/amo/

Original Article

Assessment of a New Elbow Joint Positioning Method Using Area Detector Computed Tomography

Takuya Akagawa[a,b*], Ryohei Fukui[c], Katsuhiro Kida[c], Ryutaro Matsuura[c], Makoto Shimada[d], Mitsuhiro Kinoshita[e], Yoko Akagawa[e], and Sachiko Goto[c]

Departments of [a]Radiological Technology, [e]Radiology, Tokushima Red Cross Hospital, Komatsushima, Tokushima 773-8502, Japan,
[b]Department of Radiological Technology, Graduate School of Health Sciences,
[c]Department of Radiological Technology, Faculty of Health Sciences, Okayama University, Okayama 700-8558, Japan,
[d]Department of Radiology, Osaka International Cancer Institute, Osaka 541-8567, Japan

We propose a sitting position that achieves both high image quality and a reduced radiation dose in elbow joint imaging by area detector computed tomography (ADCT), and we compared it with the 'superman' and supine positions. The volumetric CT dose index (CTDIvol) for the sitting, superman, and supine positions were 2.7, 8.0, and 20.0 mGy and the dose length products (DLPs) were 43.4, 204.7, and 584.8 mGy • cm, respectively. In the task-based transfer function (TTF), the highest value was obtained for the sitting position in both bone and soft tissue images. The noise power spectrum (NPS) of bone images showed that the superman position had the lowest value up to approx. 1.1 cycles/mm or lower, whereas the sitting position had the lowest value when the NPS was greater than approx. 1.1 cycles/mm. The overall image quality in an observer study resulted in the following median Likert scores for Readers 1 and 2: 5.0 and 5.0 for the sitting position, 4.0 and 3.5 for the superman position, and 4.0 and 2.0 for the supine position. These results indicate that our proposed sitting position with ADCT of the elbow joint can provide superior image quality and allow lower radiation doses compared to the superman and supine positions.

Key words: area detector computed tomography, elbow joint, sitting position, dose reduction, image quality assessment

Bone and joint computed tomography (CT) scans are commonly performed for various primary objectives including multiple trauma screening, detailed fracture investigation, surgery indications, surgical support imaging, and postoperative assessments [1,2]. Cone-beam CT (CBCT) has been used in this field, and specific CBCT has been developed for bone and joint diagnostic imaging and dentistry [3-5]. Although CBCT is a conventional technique, with the advent of area detector computed tomography (ADCT) in 2007 which provides 160 mm in the Z-axis direction imaging in the single-rotation non-helical mode, it became possible to obtain highly detailed data in a shorter time. This enabled the imaging of a single organs in one rotation using ADCT, and various types of imaging particularly in the head and cardiac regions are now being performed [6,7]. The selectability of non-helical and helical imaging modes in ADCT enables the optimal use in accord with the imaging range and purpose [8].

Helical-method CT (helical CT) has traditionally

Received October 16, 2023; accepted December 4, 2023.
*Corresponding author. Phone: +81-885-32-2555; Fax: +81-885-32-6350
E-mail: th_sl_f_jpn@yahoo.co.jp (T. Akagawa)

Conflict of Interest Disclosures: No potential conflict of interest relevant to this article was reported.

been used for imaging multiple bone and joint areas. The application of ADCT has been reported for the dynamic imaging of the lower limbs [9], with limited applications in the elbow region (which is evaluated primarily with helical CT and CBCT) [10]. After trauma, elbow dislocations and fractures are common, particularly in children [11]. The diagnostic procedure for elbow dislocations and fractures involves performing simple radiographic imaging to diagnose bone fractures. In cases of fracture patterns with a high degree of displacement, and when an occult fracture or radial head fracture is suspected, helical CT scans must be added for further assessment and surgical planning [12].

The greatest problem in elbow joint imaging, which is thought to present the most difficult positioning among CT examinations of bone and joint areas, is the overlapping of the elbow with other areas. The superman position (in which the affected upper limb is raised in a prone position) is performed in imaging of the elbow joint by helical CT to avoid overlap with other regions and to realize both high image quality and a low radiation dose, in the same manner as wrist imaging [13]. However, we have encountered patients with elbow injuries and impaired shoulder mobility, as well as many older individuals who have difficulty maintaining the superman position. The partial overlap of the elbow joint with the head worsens the image quality during imaging with the upper limb raised in a supine position. In the supine position with the upper limb hanging down, the elbow joint will be completely overlapped by the torso, increasing the patient's radiation exposure and degrading the image quality. A helical CT evaluation of the elbow joint thus has numerous disadvantages, including poor image quality despite the considerable exposure of the patient, and unnecessary exposure to other areas.

Limb-specific CBCT permits a comfortable position for patients with physical disability or pain [10]. However, it does have drawbacks as the field of view (FOV) is limited, motion artifacts are produced due to the prolonged imaging time, and a qualitative assessment of soft tissue lesions is not possible due to the inability to measure CT values [14, 15]. In the present study, we propose a sitting position that easily achieves both high image quality and low exposure in imaging of the elbow joint by ADCT. We evaluated the use of this position and compared it with the conventional superman and supine positions.

Patients and Methods

Current positioning. The currently used position for imaging the elbow joint is the superman position. This method is used for patients who can raise their arms but have difficulty maintaining a seated position. The superman position involves extending the elbow joint of the examined side in the prone position, which minimizes head overlap. However, fracture pain might make this pose difficult to maintain in the prone position. In this study, we defined the superman position as the position in which the arm of the examined side is raised in the prone or supine position (Fig. 1A).

We used the supine position as a comparison. The supine position is employed for patients who have difficulty raising the arm due to pain or difficulty maintaining a position with the arm raised. In the supine position, the extended arm with the elbow joint is fixed to the side of the torso and imaged simultaneously with the torso while instructing the patient to hold their breath (Fig. 1B).

Proposed positioning. We propose the use of the sitting position, which is designed for patients who can maintain a seated position with their arms raised. For the evaluation of the utility of the sitting position, three lines were set at 80-mm intervals in the center of the top of a cardboard box measuring 280 mm wide × 330 mm high × 380 mm deep. The cardboard box was set inside the gantry of the ADCT system described below, and a laser pointer was aligned with the center line. Imaging was performed with the patient sitting on the examination table with the elbow arranged on the cardboard box, palm facing upward to the extent possible (Fig. 1C). The sitting position enables imaging of the elbow joint at the isocenter, without overlap with other body parts.

Patients. A total of 54 consecutive patients who underwent elbow joint CT in one of these positions between October 2012 and February 2023 at Tokushima Red Cross Hospital (Tokushima, Japan) were included in the study. There were 18 patients for each of the three positions (sitting, superman, and supine), and consecutive cases were collected within the study period. All patients also had either a dislocation and fracture suspected based on radiographs or a close examination and follow-up of fractures.

Table 1 shows the breakdown of the patients examined in each position. This study was approved by the Tokushima Red Cross Hospital Ethics Committee

(Approval no. 461).

CT scanner and scan parameters. For all 54 patients, imaging was performed using the Aquilion ONE V4.74 JR016 (Canon Medical Systems, Tochigi, Japan). This system has an ADCT apparatus in which 0.5-mm detectors are mounted in 320 rows. Table 2 shows the scan parameters for each position. We used the volumetric CT dose index (CTDIvol) and dose length product (DLP) as indicators of radiation exposure at each position. These were accessed from the console associated with the CT.

Image reconstruction parameters. For the reconstruction technique, we used AIDR3D, an adaptive iterative dose reduction technique. Outputs for the observational study described below were in the form of bone and soft tissue conditions. For the bone kernels, the "weak" dose reduction level was used for FC31 and AIDR3D, while for the soft tissue kernels, the "mild" dose reduction level was used for FC04 and AIDR3D, respectively. The matrix size was 512×512 pixels, and the slice thickness and interval were 0.5 mm.

We considered the forearm to the upper arm of the imaging area centered on the elbow joint to be the minimum display field of view (DFOV). Multiplanar

Fig. 1 The positions for image acquisition using area detector computed tomography (ADCT): **A**, the superman position in a prone position with the examined arm raised; **B**, the supine position with the elbow joint at the side of the torso, and **C**, the proposed sitting position.

Table 1 Cases in each of the imaging positions

Position	Sitting position (n = 18)	Superman position (n = 18)	Supine position (n = 18)
Age (mean ± SD* y/o)	53.2 ± 28.6	62.8 ± 28.2	71.2 ± 26.0
Sex (men/women)	9/9	7/11	9/9

*Standard deviation.

Table 2 Scan parameters for each position in 18 patients

Position	Sitting position	Superman position	Supine position
Scan mode	Non-helical	Helical	Helical
Collimation [mm]	320 × 0.5	80 × 0.5	80 × 0.5
Tube voltage [kVp]	100	120	120
Tube current [mA]	40	10 to 550*	10 to 550*
Rotation time [s]	0.5	0.5	0.5
Pitch factor	–	0.638	0.638

*Auto exposure control (AEC) setting parameters were slice thickness 3 mm, standard deviation range of 8.0～11.0 HU with CT-AEC.

reconstruction (MPR) images were created on the console associated with the CT system, creating axial, coronal, and sagittal images with a slice thickness of 2 mm for the bone images and axial images with a slice thickness of 3 mm for the soft tissue images.

Task-based image quality analysis. The images corresponding to the elbow joint at each position were physically assessed using the task-based transfer function (TTF) and the noise power spectrum (NPS). Figure 2 shows an overview of the handmade phantom. We affixed a cylindrical phantom of CT values modeling bone at the center of an 80-mm cylindrical plastic container, approximating an elbow joint. The cylindrical phantom was the 1456 HE Inner Bone (Electron Density Relative to Water 1.16, 120 kV, and approx. 450 HU) solid insert associated with the Advanced Electron Density Phantom (Sun Nuclear Corp., Melbourne, FL, USA). We filled the inside of a plastic container with water and used this as the phantom for the image quality assessment. Figure 3 shows the arrangement of the phantom for the image quality assessment, which modeled each position.

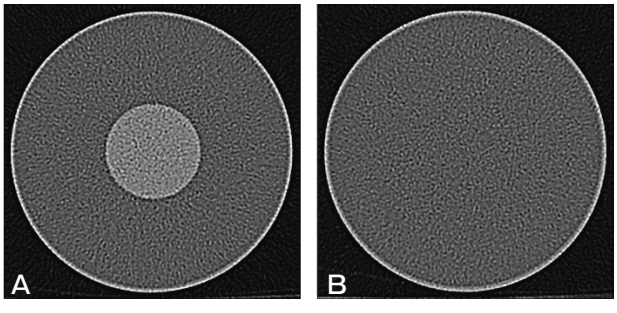

Fig. 2 CT images of the image-quality assessment phantom. These are the measurement ranges in the slices used in this study for (A) the task-based transfer function (TTF) and (B) the noise power spectrum (NPS).

The sitting position was considered the state in which the phantom was arranged on the cardboard box so that the center of the phantom matched the isocenter (Fig. 3A). When modeling the superman position, we arranged the phantom on the examination table so that the center of the phantom was 100 mm off-center from the isocenter (Fig. 3B). In the case of the supine position, we filled both the inner and outer tubs of a WAC thoracic/abdominal X-ray water phantom (300 mm wide × 450 mm high × 200 deep, Kyoto Kagaku, Kyoto, Japan), arranged the phantom center so that it matched the isocenter, and arranged the image quality assessment phantom adjacent to it (Fig. 3C). Table 3 shows the respective scan parameters.

The CTDIvol was used to calculate the radiation dose for imaging in each position. The image quality assessment phantom was determined with reference to the CTDIvol when imaging cases in each position. The CTDIvol values for the sitting and supine positions were chosen to match the mean CTDIvol of 18 patients in each respective group in which elbow joint imaging was

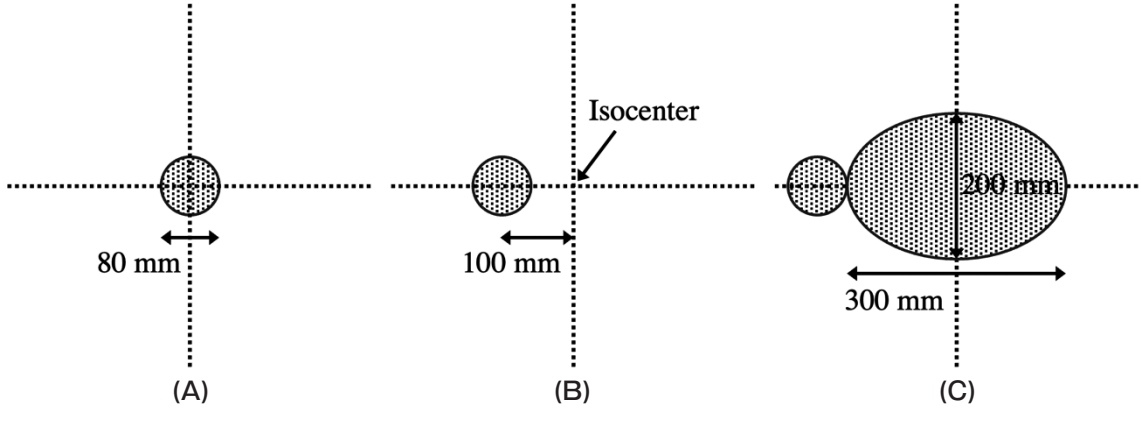

Fig. 3 Arrangement of the image-quality assessment with phantom modeling for each of the three positions: A, the sitting position where the center of the phantom was arranged to match the isocenter; B, the superman position, in which the center of the phantom was arranged at 100 mm off-center of the isocenter, and C, the supine position where a thoracic/abdominal X-ray phantom filled with water in both the inner and outer tubs was arranged to match the isocenter of the X-ray water phantom, and the image quality assessment phantom was arranged adjoining it.

Table 3 Scan parameters of the task-based image quality analysis for each position

Position	Sitting position	Superman position	Supine position
Scan mode	Non-helical	Helical	Helical
Collimation [mm]	320 × 0.5	80 × 0.5	80 × 0.5
Tube voltage [kVp]	100	120	120
Tube current [mA]	40	70	260
Rotation time [s]	0.5	0.5	0.5
Pitch factor	–	0.638	0.638
CTDIvol [mGy]	2.7 (16 cm)*	5.2 (32 cm)*	20.2 (32 cm)*

*CTDIvol for 16 cm and 32 cm diameter PMMA dosimetry phantom.

performed at each respective position. The superman position CTDIvol was treated as an imaging condition, and we used the mean CTDIvol of 11 of the 18 patients who underwent elbow joint imaging in the superman position for whom the head did not overlap the imaging area. The image reconstruction conditions were matched with the clinical imaging, and all of the images had a 160-mm DFOV.

In the image quality assessment using the phantom, the imaging was repeated 20 times under the same conditions to obtain images of the same slice position. The software program CTmeasureBasic ver. 0.97b2 (Japanese Society of CT Technology, Hiroshima, Japan) was used to calculate the TTF and NPS values. The circular edge method was used for the TTF, and the radial frequency method was used for the NPS. The TTF was calculated by arithmetically averaging the 20 slice images of the same cylindrical phantom. The NPS was calculated for each of the images of the same slice obtained from 20 scans of the water-only position where there was no cylindrical phantom. These individual NPS values were averaged and used as the final NPS.

Observer study. We conducted an observer study to assess the elbow joint at each position objectively. The observers were two radiologists (Reading experience: Reader 1: 15 years, Reader 2: 16 years). The assessment for the observations was performed using a RadiForce RX660 diagnostic monitor (EIZO, Ishikawa, Japan). First, to identify assessment criteria for the observers, we performed a practice observer study with a dataset different from that used for the assessment. The cases were displayed one by one on the monitor, and the observers assessed whether the image quality of each case was sufficient for diagnosis. No limits were set for the observation time or the distance from the monitor. the observers were allowed to change the window width (WW) and window level (WL) freely. The images' overall quality was assessed using a 5-point Likert scale (5 = excellent, 4 = very good, 3 = good, 2 = fair, 1 = poor). Bone and soft tissue artifacts and image noise were further assessed using a 5-point Likert scale (5 = minimal artifacts or noise, 4 = little artifacts or noise, 3 = moderate artifacts or noise, 2 = considerable artifacts or noise, 1 = strong artifacts or noise).

Statistical analyses. The CTDIvol and DLP values at each position were analyzed, and the observer study results were evaluated by an analysis of variance (ANOVA) and multiple comparisons. The Tukey method was adopted for the multiple comparisons. The significance level was set at $p < 0.05$. SPSS Statistics (ver. 21.0 for Windows, IBM, Armonk, NY, USA) was used for the statistical analyses.

Results

Radiation dose. Figure 4 shows the CTDIvol and DLP values for each imaging position in the patient study. The CTDIvol values for the sitting, superman, and supine positions were 2.7 ± 0.0 mGy (phantom dia. for the CTDI measurement: 16 cm, same below), 8.0 ± 4.3 mGy (32 cm), and 20.0 ± 7.2 mGy (32 cm), and the DLP values were 43.4 ± 0.0 mGy • cm, 204.7 ± 116.6 mGy • cm, and 584.8 ± 315.8 mGy • cm, respectively. The mean CTDIvol and DLP values for 11 of the 18 patients who underwent elbow imaging in the superman position, in which the head did not overlap the imaging area, were 5.2 ± 1.9 mGy (32 cm) and 139.9 ± 86.6 mGy • cm, and the corresponding values for 7 of the 18 patients who underwent elbow imaging in the overlapping superman position were 12.3 ± 3.0 mGy (32 cm) and 306.5 ± 78.9mGy • cm,

respectively.

The sitting position exhibited significantly lower CTDIvol and DLP values compared to the superman and supine positions.

Task-based image quality analysis. The TTF and NPS values for the bone and soft tissue images obtained using the handmade phantom are depicted in Fig. 5 and 6. Regarding the TTF, the sitting position exhibited the highest values in both bone and soft tissue images. The superman position resulted in a lower TTF for both, and the supine position provided the lowest values. The TTF peak for bone images shifted to a low frequency with the change from the sitting position to the superman position and supine position. Concerning the NPS, the supine position exhibited a relatively high value in the frequency components except around 0.5-1.1 cycles/mm. Although the superman position exhibited the lowest bone-image NPS values up to about ≤1.1 cycles/mm, the sitting position had the lowest at approx. ≥1.1 cycles/mm. The sitting position had the highest value (approx. 0.6-0.95 cycles/mm). For the soft tissue images, the NPS was lowest in the sitting position at approx. ≥1.1 cycles/mm.

Observer study. In the observer study of overall image quality, no case with a score of 1 was observed, representing the lowest assessment. Reader 1 and Reader 2 determined that 5.6% and 55.5% of the images obtained with the patients in the supine position were

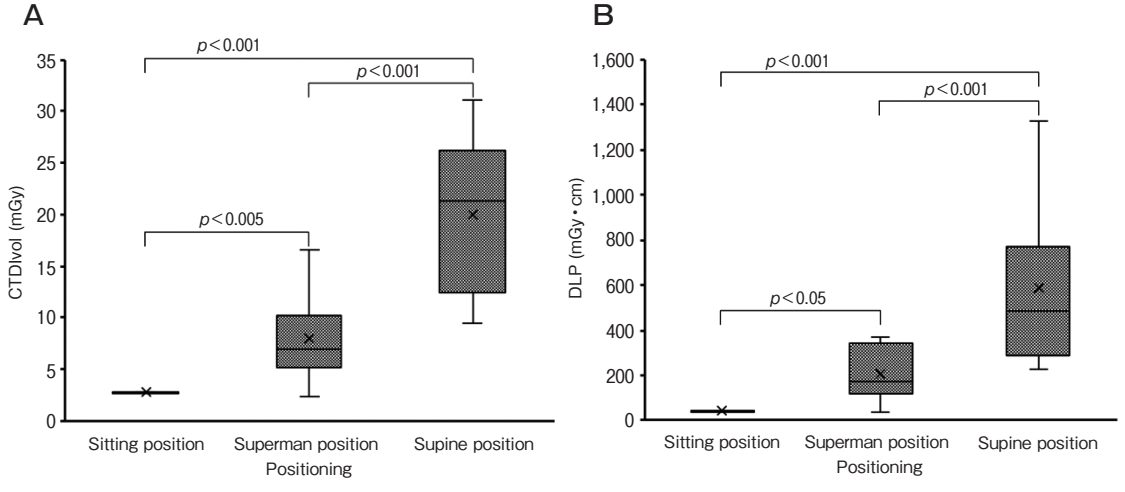

Fig. 4 The CTDIvol and the dose length product (DLP) for each imaging position in 18 patients. (A) The CTDIvol and (B) the DLP for each position. "X" indicates the mean value. The superman position is the mean value of the cases with and without head overlap.

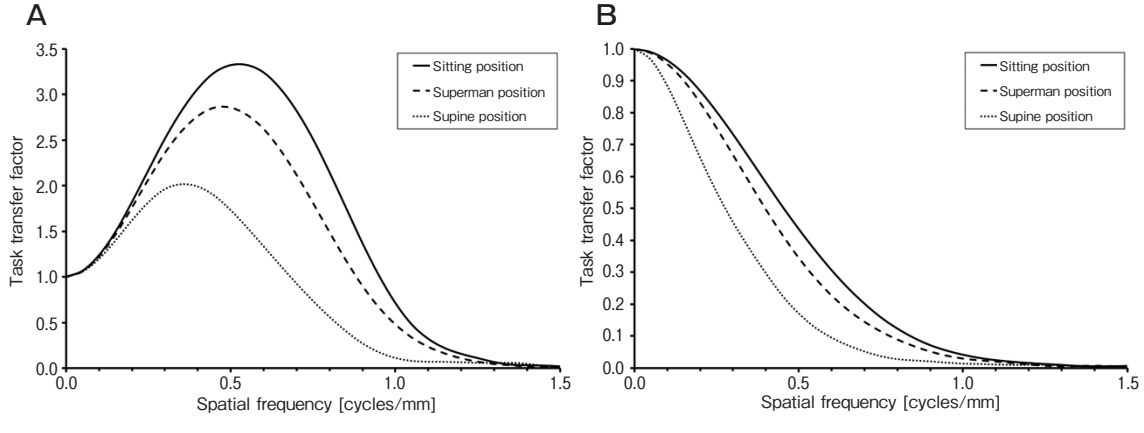

Fig. 5 Comparison of the task-based transfer function (TTF) in each position with the use of the handmade phantom. (A) Bone images and (B) soft tissue images.

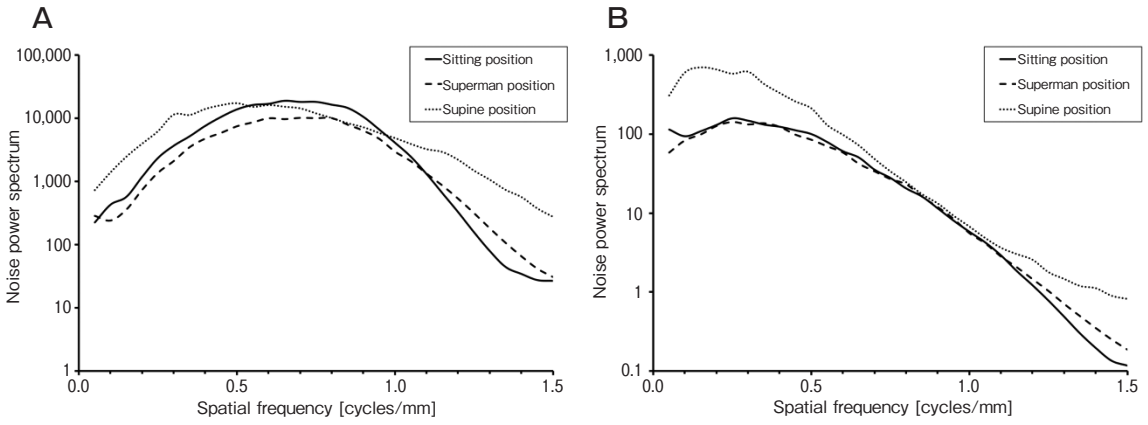

Fig. 6 Comparison of the noise power spectrum (NPS) in each position with the use of the handmade phantom. (**A**) Bone images and (**B**) soft tissue images.

insufficient for diagnostic use (Score 2). The two readers determined the overall image quality to be excellent or very good (score 5 or 4) for 100% and 100% of cases in the sitting position, 72.2% and 50.0% in the superman position, and 61.1% and 27.8% in the supine position. The median Likert scores for Readers 1 and 2 were 5.0 and 5.0 in the sitting position, 4.0 and 3.5 in the superman position, and 4.0 and 2.0 in the supine position. The results of our analyses demonstrated that the image quality of the sitting position was significantly superior to those of the other positions.

Figure 7 shows typical axial, coronal, and sagittal MPR images for the sitting, superman, and supine positions, and Table 4 provides the detailed results of the observer study. MPR images with Reader 1 and Reader 2 in the sitting position (with an overall image quality ratings at 4.0 and 4.0) are presented in Fig. 8.

The observer study's image noise and artifacts results are summarized in Table 5. The results of our analyses demonstrated that the image noise and artifacts of the sitting position was significantly superior to those of the other positions.

Discussion

We have introduced a sitting position for elbow joint CT evaluations using non-helical ADCT imaging. We used this approach to compare the radiation doses and image quality with the superman and supine positions during helical ADCT imaging. In the sitting position, the mean values of CTDIvol and DLP were 1/3 and 1/4.7 those of the superman position and 1/7.4 and 1/13.5 those of the supine position. An observer study by two radiologists revealed that the sitting position produced better images than the superman and supine positions. In the TTF assessments of bone and soft tissue images, the sitting position had the highest values across all frequencies. The sitting position exhibited the lowest values when the NPS of bone images was approx. ≥ 1.1 cycles/mm. In the observation of fine bone structures, the sitting position exhibited little noise while maintaining high resolution. This result indicates that the sitting position had less bone and soft tissue noise and fewer artifacts compared to the superman and supine positions.

Although trauma imaging of the elbow joint focuses mainly on bone imaging, for fracture identification, it is also important to have minimal noise and artifacts in soft tissue, especially in cases of occult fractures with hematoma [16]. In addition, CT examinations require that the patient's body posture be maintained during imaging, and body movement will cause blurring in the image. Position stability is thus required to reduce the patient's pain and to help the patient maintain a body position. Encouraging the patients' cooperation while considering their pain and obtaining the best maintainable body position enable a reduction of motion artifact in imaging. Moreover, the existence of objects of high X-ray absorbency should be avoided within the imaging range. High-absorbency objects are associated with increased streak artifacts and radiation doses [17]. Fine structural observations also require sufficient spatial resolution.

To the greatest degree possible, elbow joint imaging

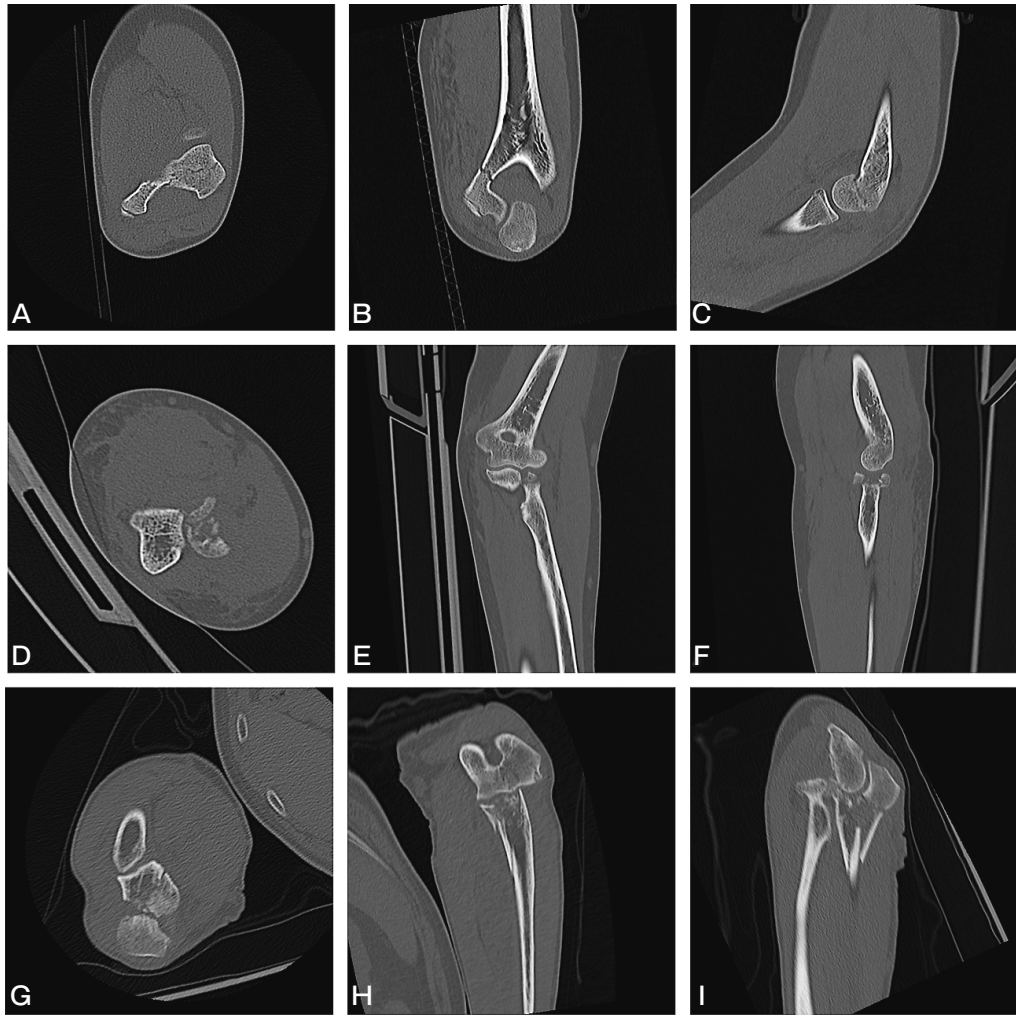

Fig. 7 Axial, coronal, and sagittal images in each position. (**A**-**C**) sitting position, (**D**-**F**) superman position, and (**G**-**I**) supine position. The CTDIvol values for the sitting, superman, and supine positions were 2.7 mGy (16 cm), 9.7 mGy (32 cm), and 23.3 mGy (32 cm) and the DLP values were 43.4 mGy•cm, 331.1 mGy•cm, and 584.4 mGy•cm, respectively. The overall image quality scores for Reader 1 and Reader 2 were 5.0 and 5.0 in the sitting position, 4.0 and 3.0 in the superman position, and 4.0 and 3.0 in the supine position.

Table 4 Results of the observer study in which two radiologists participated, using patient images

	Score	Sitting position (No. of case [%])		Superman position (No. of case [%])		Supine position (No. of case [%])	
		Reader1	Reader2	Reader1	Reader2	Reader1	Reader2
Overall image quality	5	17 (94.4)	11 (61.1)	7 (38.9)	2 (11.1)	5 (27.8)	–
	4	1 (5.6)	7 (38.9)	6 (33.3)	7 (38.9)	6 (33.3)	5 (27.8)
	3	–	–	5 (27.8)	8 (44.4)	6 (33.3)	3 (16.7)
	2	–	–	–	1 (5.6)	1 (5.6)	10 (55.5)
	1	–	–	–	–	–	–
	Median	**5.0**	**5.0**	**4.0**	**3.5**	**4.0**	**2.0**

Image quality ordinal score: 5 = excellent, 4 = very good, 3 = good, 2 = fair, 1 = poor.

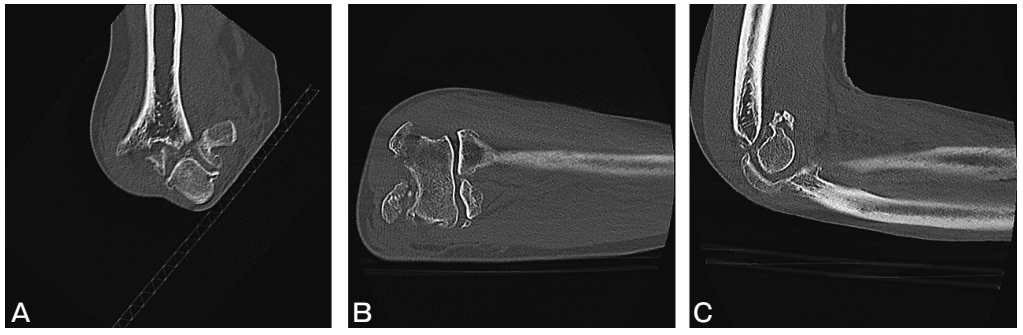

Fig. 8 Sitting position images in which the elbow joint extension was insufficient. (**A**) axial, (**B**) coronal, and (**C**) sagittal views. The CTDIvol was 2.7 mGy (16 cm) and the DLP was 43.4 mGy•cm. The overall image quality scores for Reader 1 and Reader 2 were 4.0 and 4.0.

Table 5 Assessment of image noise and artifacts in the bone and soft tissue evaluated in the observer study using patient images

	Score	Sitting position (No. of case [%])		Superman position (No. of case [%])		Supine position (No. of case [%])	
		Reader1	Reader2	Reader1	Reader2	Reader1	Reader2
Noise in bone	5	16 (88.9)	14 (77.8)	6 (33.3)	4 (22.2)	4 (22.2)	–
	4	2 (11.1)	4 (22.2)	6 (33.3)	5 (27.8)	6 (33.3)	5 (27.8)
	3	–	–	6 (33.3)	8 (44.4)	8 (44.4)	3 (16.7)
	2	–	–	–	1 (5.6)	–	10 (55.5)
	1	–	–	–	–	–	–
	Median	**5.0**	**5.0**	**4.0**	**3.5**	**4.0**	**2.0**
Noise in soft tissue	5	4 (22.2)	–	–	–	–	–
	4	13 (72.2)	15 (83.3)	8 (44.4)	7 (38.9)	2 (11.1)	1 (5.6)
	3	1 (5.6)	3 (16.7)	8 (44.4)	7 (38.9)	13 (72.2)	7 (38.9)
	2	–	–	2 (11.1)	4 (22.2)	3 (16.7)	9 (50.0)
	1	–	–	–	–	–	1 (5.6)
	Median	**4.0**	**4.0**	**3.0**	**3.0**	**3.0**	**2.0**
Artifacts in bone	5	11 (61.1)	15 (83.3)	3 (16.7)	5 (27.8)	–	3 (16.7)
	4	7 (38.9)	3 (16.7)	10 (55.5)	7 (38.9)	10 (55.5)	4 (22.2)
	3	–	–	5 (27.8)	4 (22.2)	8 (44.4)	7 (38.9)
	2	–	–	–	2 (11.1)	–	4 (22.2)
	1	–	–	–	–	–	–
	Median	**5.0**	**5.0**	**4.0**	**4.0**	**4.0**	**3.0**
Artitacts in soft tissue	5	1 (5.6)	2 (11.1)	–	1 (5.6)	–	–
	4	14 (77.8)	12 (66.7)	8 (44.4)	8 (44.4)	1 (5.6)	2 (11.1)
	3	2 (11.1)	3 (16.7)	6 (33.3)	2 (11.1)	11 (61.1)	5 (27.8)
	2	1 (5.6)	1 (5.6)	4 (22.2)	7 (38.9)	6 (33.3)	10 (55.5)
	1	–	–	–	–	–	1 (5.6)
	Median	**4.0**	**4.0**	**3.0**	**3.5**	**3.0**	**2.0**

Image quality ordinal score: 5 = minimal artifacts or noise, 4 = little artifacts or noise, 3 = moderate artifacts or noise, 2 = considerable artifacts or noise, 1 = strong artifacts or noise.

should be performed at the isocenter because the TTF decreases in bone and soft tissue imaging in the superman position compared to the sitting position [18]. Our present findings demonstrated that the supine position further reduced the TTF much more than the superman position. In addition to the supine position reaching 190 mm off-center, the greater increase in the tube current and the enlargement of the X-ray tube focal spot due to the high absorption of X-rays by the trunk in the X-Y plane may have reduced the TTF [19]. The TTF may have been influenced by AIDR3D noise reduction processing, an iterative reconstruction technique that increases with streak artifacts and noise [20, 21].

The sitting position we have proposed achieves all of the conditions demanded by the elbow joint imaging described above. A further advantage of the sitting position is the high reproducibility of the MPR images created. Accurate MPR creation is required in both the determination of surgical indications and temporal observations [16]. MPR reproducibility is important because the differences in the MPR angle between image creators affects both the diagnosis and treatment efficacy. As with plain radiographic imaging, mid-position imaging maximizes reproducibility. Sitting with the elbow joint supported by a cardboard box makes imaging in the mid-position simple and reproducible, similar to plain radiographic imaging.

Because imaging in the sitting position using ADCT omits the need for localizer radiographs taken first in conventional CT imaging, it is possible to further reduce patients' exposure and shorten the imaging time [22]. Although the CT-auto exposure control (AEC) that is used in general CT imaging modulates the tube current in the Z-axis direction matched to the image quality set after calculating the thickness from the localizer radiographs, it is not possible to use CT-AEC for imaging with the sitting position [23]. Therefore, even though it is necessary to set the scan parameters on the user side, the elbow joint thickness is more uniform, and even with a fixed tube current, the image quality is similar at the upper arm and forearm. In the superman position, non-helical imaging works; however, if the patient's head partially overlaps the elbow joint, the imaging dose must be considerably increased, resulting in an excessive radiation dose at the locations not overlapped by the head. Helical CT imaging is thus suitable for the superman position, where the head might overlap.

Our present results showed that the DLP reduction rate was greater in the sitting position than the CTDIvol reduction rate, and we speculated that this is due to the different methods of determining the imaging area in non-helical and helical imaging. The maximum range of non-helical imaging in which ADCT is used is 160 mm. However, as helical CT imaging may be set at any imaging range, the maximum range will always be longer. This is thought to be because the imaging technicians subconsciously tend to include a longer imaging area that encompasses the entire affected part of the patient. The present observers observed longer imaging areas in patients for whom the scores were particularly low. When the imaging range is longer or the Z-axis direction is longer, shrinking the image to display the entire affected area during the creation of coronal and sagittal image may reduce the scores.

Although there were multiple cases in which the sitting position had lower scores than the other positions in this study, in those cases the extension of the elbow joint was insufficient (Fig. 8). When the extension of the elbow joint is insufficient, the subject thickness in the X-Y plane will become thicker due to the forearm maintaining an angle in the Z-axis direction, resulting in an inadequate dose exposure. In cases in which a patient cannot fully extend the elbow joint due to it being fixed by a splint or due to pain, it is necessary to adjust the scan parameters.

We also found that due to the omission of localizer radiographs, the workflow was greatly improved, and the positioning time was significantly reduced for ambulatory patients of all ages. We believe that sitting is the best position for elbow joint imaging because the scanning time was very short (0.5 sec). This positioning is also applicable to pediatric patients with small bodies who have difficulty maintaining their body position and can be held by their guardians.

Limitations of this study include the measured TTF and NPS values exhibiting characteristics of axial imaging in the basic assessment method, which was limited to the X-Y plane, with no assessment made in the Z-axis direction. Position assignments may be biased due to the severity of a patient's injury and the patient's body size at the time of the scan. However, our observer study did not assess the severity of the patients' injuries, and there was thus no influence of the severity. Additional study limitations are that there were only two radiologists serving as observers, no orthopedists were

included, and the study was a single-center, retrospective investigation.

The sitting position that we propose, using ADCT for elbow joint imaging, produced superior image quality compared to both the superman and supine positions, in which helical imaging was used. Because the localizer radiographs were omitted, the exposure and examination times were also substantially shortened. In addition to achieving dose reductions of 79% compared to the superman position and 93% compared to the supine position, the use of the sitting position made it possible to eliminate direct X-ray exposure to areas other than the elbow joint.

In conclusion, our proposed sitting position with ADCT of the elbow joint will provide superior image quality and enable lower radiation doses compared to the superman and supine positions. The elbow joint imaging technique proposed in this study thus merits future consideration as the standard for elbow joint imaging.

References

1. Huber-Wagner S, Lefering R, Qvick LM, Körner M, Kay MV, Pfeifer KJ, Reiser M, Mutschler W and Kanz KG: Effect of whole-body CT during trauma resuscitation on survival: a retrospective, multicentre study. Lancet (2009) 373: 1455–1461.
2. Pretorius ES and Fishman EK: Volume-rendered three-dimensional spiral CT: musculoskeletal applications. Radiographics (1999) 19: 1143–1160.
3. Miracle AC and Mukherji SK: Conebeam CT of the head and neck, part 2: clinical applications. AJNR Am J Neuroradiol (2009) 30: 1285–1292.
4. Koong B: Cone beam imaging: is this the ultimate imaging modality? Clin Oral Implants Res (2010) 21: 1201–1208.
5. Carrino JA, Al Muhit A, Zbijewski W, Thawait GK, Stayman JW, Packard N, Senn R, Yang D, Foos DH, Yorkston J and Siewerdsen JH: Dedicated cone-beam CT system for extremity imaging. Radiology (2014) 270: 816–824.
6. Orrison WW Jr, Snyder KV, Hopkins LN, Roach CJ, Ringdahl EN, Nazir R and Hanson EH: Whole-brain dynamic CT angiography and perfusion imaging. Clin Radiol (2011) 66: 566–574.
7. Takamura K, Fujimoto S, Kawaguchi Y, Kato E, Aoshima C, Hiki M, Kumamaru KK, and Daida H: The usefulness of low radiation dose subtraction coronary computed tomography angiography for patients with calcification using 320-row area detector CT. J Cardiol (2019) 73: 58–64.
8. Roy C, Quin R, Labani A, Leyendecker P, Mertz L and Ohana M: Wide volume versus helical acquisition using 320-detector row computed tomography for computed tomography urography in adults. Diagn Interv Imaging (2018) 99: 653–662.
9. Gondim Teixeira PA, Formery AS, Jacquot A, Lux G, Loiret I, Perez M and Blum A: Quantitative Analysis of Subtalar Joint Motion With 4D CT: Proof of Concept With Cadaveric and Healthy Subject Evaluation. AJR Am J Roentgenol (2017) 208: 150–158.
10. Grunz JP, Weng AM, Kunz AS, Veyhl-Wichmann M, Schmitt R, Gietzen CH, Pennig L, Herz S, Ergün S, Bley TA and Gassenmaier T: 3D cone-beam CT with a twin robotic x-ray system in elbow imaging: comparison of image quality to high-resolution multidetector CT. Eur Radiol Exp (2020) 4: 52.
11. Subasi M, Isik M, Bulut M, Cebesoy O, Uludag A and Karakurt L: Clinical and functional outcomes and treatment options for paediatric elbow dislocations: Experiences of three trauma centres. Injury (2015) 46: S14–18.
12. Sheehan SE, Dyer GS, Sodickson AD, Patel KI and Khurana B: Traumatic elbow injuries: what the orthopedic surgeon wants to know. Radiographics (2013) 33: 869–888.
13. Suresh SP and Ninan T: Computed tomography of hand and wrist; in Imaging of the hand and wrist – techniques and applications, Davies AM, Grainger AJ and James SJ eds, 1st Ed, Springer, Berlin (2013) pp 23–36.
14. Posadzy M, Desimpel J and Vanhoenacker F: Cone beam CT of the musculoskeletal system: clinical applications. Insights Imaging (2018) 9: 35–45.
15. Nardi C, Molteni R, Lorini C, Taliani GG, Matteuzzi B, Mazzoni E and Colagrande S: Motion artefacts in cone beam CT: an in vitro study about the effects on the images. Br J Radiol (2016) 89: 20150687.
16. Haapamaki VV, Kiuru MJ and Koskinen SK: Multidetector computed tomography diagnosis of adult elbow fractures. Acta Radiol (2004) 45: 65–70.
17. Barrett JF and Keat N: Artifacts in CT: recognition and avoidance. Radiographics (2004) 24: 1679–1691.
18. Rubert N, Szczykutowicz T and Ranallo F: Improvement in CT image resolution due to the use of focal spot deflection and increased sampling. J Appl Clin Med Phys (2016) 17: 452–466.
19. Grimes J, Duan X, Yu L, Halaweish AF, Haag N, Leng S and McCollough C: The influence of focal spot blooming on high-contrast spatial resolution in CT imaging. Med Phys (2015) 42: 6011–6020.
20. Samei E and Richard S: Assessment of the dose reduction potential of a model-based iterative reconstruction algorithm using a task-based performance metrology. Med Phys (2015) 42: 314–323.
21. Tsuda N and Mitsui K: Evaluation of Noise Properties at Nonuniformity Area and Resolution Properties of CT Image Using Iterative Reconstruction Method. Nihon Hoshasen Gijutsu Gakkai Zasshi (2022) 78: 809–818.
22. Schmidt B, Saltybaeva N, Kolditz D and Kalender WA: Assessment of patient dose from CT localizer radiographs. Med Phys (2013) 40: 084301.
23. Söderberg M and Gunnarsson M: Automatic exposure control in computed tomography – an evaluation of systems from different manufacturers. Acta Radiol (2010) 51: 625–634.